Kaolin-Calcium Carbonate-Titanium Dioxide (K-C-T) Composites for Decolourisation of Reactive Dye Effluent

[1]S. Tharakeswari, [2]D. Saravanan, [3]Ashwini K Agrawal and [4]Manjeet Jassal
[1]*Department of Textile Technology, PSG College of Technology, Coimbatore 641004, India*.
[2]*Department of Textile Technology, Kumaraguru College of Technology, Coimbatore 641049, India*.
[3,4]*Department of Textile Technology, Indian Institute of Technology, New Delhi 110016, India*.
thara.sundar@gmail.com*

(Received on 16th May 2022, accepted in revised form 19 September 2022)

Summary: Synthetic dyes in textile effluents cause serious environmental and aquatic life hazards if discharged in water bodies without decolorisation and removal of toxic substances. Efforts have been made to produce composites of Kaolin-$CaCO_3$-TiO_2 (K-C-T Composite) using the proportions of 1:1:1, 1:2:1 and 1:1:2 through calcination and assess their potential to remove colour from the effluents of Reactive Black 5 dye. Photocatalytic-composite adsorbent has been characterised for morphological structure, phase determination, band gap and Fourier-transform infrared spectroscopy for colour removal and dye decomposition studies. Studies show a maximum of 82% and 80% colour removal efficiency using 1:1:1 and 1:1:2 proportions of K-C-T composites respectively, calcined at 1000 ℃. Surface area of the composite samples, state of titanium dioxide in the composite and band gap of the composite influences the colour removal from the effluent significantly.

Keywords: Physicochemical, Calcination, Composite, Decolourisation, Photocatalyst.

Introduction

Azo dyes, widely used in textile industries, have been a threat to all human beings and other living organisms due to their tendency to react and generate carcinogenic byproducts including aromatic amines [1]. Reactive Black 5 is one such dye that contains diazo group in its structure as a chromophore and is abundantly used dye in the textile processing [2–4]. Oxidation treatments using hydrogen peroxide, chlorine and other Advanced Oxidative Processes which employ ultraviolet rays, ozone or photocatalysts are highly favoured by the industries in the treatment of effluents [5–7] to reduce the impact on the ecological systems [8,9].

Though several studies focus on the treatment of residual dyes and colourants present in the textile effluents using adsorbents [10], photocatalysts, biological reactions, solubilization, electrolytic processes, etc., the search for a sustainable and efficient process is still being explored by the researchers. Chemical methods produce huge amount of sludges, while physical methods are no longer effective since the adsorbents themselves become toxic, biological treatments require strict monitoring of optimal conditions and effective electrochemical methods require substantial investments [11–13].

Combinations of two or more methods have been studied in the recent years to overcome certain disadvantages and efficient colour removal [14,15]. Recent researches have elaborated the importance of forming chemical composites using photocatalyst and adsorbents [14,16,17]. Use of nano-photocatalysts and nano particles for treatment of dye effluents has resulted in environmental impacts including toxicity to aquatic organisms and water bodies. Hence, it is necessary to look for a sustainable solutions without affecting resources and the environment [18,19]. On this ground, the present study was designed to develop an adsorbent-cum-photocatalyst, a composite material made of kaolin ($Al_2SiO_5(OH)_4$), calcium carbonate ($CaCO_3$) and titanium dioxide (TiO_2), using calcination technique to obtain optimum surface morphology to facilitate for enhanced dye removal.

Calcination, a thermal process of materials, aids in obtaining quasi-amorphous substances by removing moisture and initiating the formation of new compounds. Thermal activation promotes phase transitions that enhance the physical and chemical properties of prepared composite [20]. Thermo-chemical changes of composites with respect to components and composite performance on decolourisation of RB5 are highlighted in the current study. Proportions of different components for KCT composite have been chosen for the current study based on the similar raw materials used in the cement manufacturing, i.e. 80% of calcium carbonate and 20% of Kaolin clay [21] so that the resulting saturated adsorbents could be safely used as an alternative material for clinkers [22] and pigment / water based

*To whom all correspondence should be addressed.

paint manufacturing [23], thereby reducing impact on the environment.

Experimental

Dye and Chemicals

Reactive Black 5 (C.I Number 20505 / CAS Number 12225-25-1- Jakazol Black BN 150) was supplied by M/s Jay Chemical Industries, India. Kaolin (K), calcium carbonate (C) and titanium dioxide (T) were purchased from Loba Chemie, SD Fine Chem and Merck India, respectively.

Preparation of composites

Composites with proportions of 1:1:1, 1:2:1 and 1:1:2, kaolin (K), calcium carbonate (C) and titanium dioxide (T), were prepared by calcination, for one hour, in a muffle furnace at temperatures 900, 1000, 1100 and 1200 °C, with a heating rate of 10 °C per minute. The proportions and temperatures were chosen considering the formation of calcium titanate and belite as a composite which is expected to contribute to photocatalytic reactions and adsorption respectively [24,25].

Preparation of dye effluent

Reactive Black 5 was used to dye the cotton fabrics (2 % on weight of the fabric) with sodium chloride (40 gram per litre) as exhausting agent and 15 gram per litre sodium carbonate (Na_2CO_3) as the fixing agent. Material to liquor ratio for dyeing was maintained at 1:40 and the dyeing was carried at 70 °C for 1 hour [26]. After dyeing, the fabric samples were removed and the dye effluent was collected for further treatment.

Treatment of dye effluent

Treatment of dye effluent was carried in an UV Chamber [27] made up of a wooden (5) box (Fig 1) with a (1) UV light source (power 8W) having wavelength of 365 nm with exhaust facility (6). Effluent samples were taken in a beaker (2) and placed on a magnetic stirrer (3) under UV light with constant stirring to promote photocatalytic reaction of composite specimens. Dye effluent was treated with 10 g of composite material per litre of effluent at pH 3, 5, 7, 9 and 11 for a duration of 2, 4 and 6 hours [28].

Characterization

X-Ray diffraction analysis

Crystallinity of the KCT composites was evaluated by X-ray diffraction. The diffraction (2θ) was carried out between 5 to 90° at a scanning speed of 4.0 deg/min. XRD result was fed into Match – Phase identification software to determine crystallite phase, crystallinity and amorphous content. Phase identification is done by Crystallography Open Database [29].

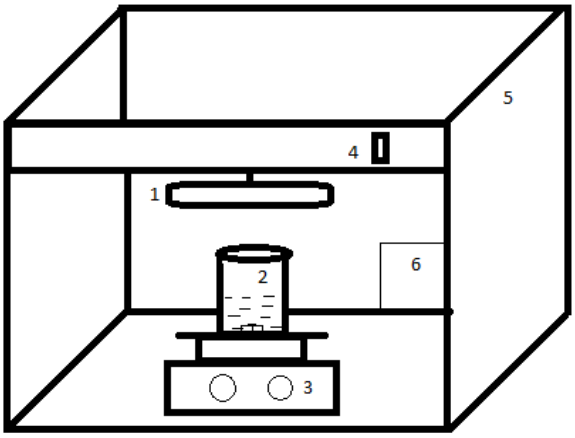

Fig. 1: UV Chamber for Effluent Treatment.

Morphology and Surface area

Morphological studies of the KCT composite samples were conducted using Field Emission Scanning Electron Microscope, capable of 0.7 nm resolution and magnification up to X1000,000 with accelerating voltage starting from 0.01 kV to 30 kV. Surface area of the composite samples were estimated using Surface Area Analyser – Quantachrome NovaWin version 11.05. Degassing of the samples was done for 6 hours at 150 °C and samples were tested under nitrogen atmosphere [30].

UV-Vis diffuse reflectance spectroscopy

Bandgaps of the composite samples were analysed using UV-Vis spectrophotometer. UV-Vis diffuse reflectance spectra were obtained using UV-vis spectrophotometer, between the wavelengths 200 to 800 nm [31]. Bandgap values of photocatalytic adsorbents were calculated using equation 1 [32].

$$Band\ gap\ (eV) = \frac{1240}{\lambda} \qquad (1)$$

where, the constant 1240 is given by hν (h – Planck's constant, ν – frequency) and λ is the wavelength.

Decolourisation analysis

Decolourisation of dye effluents was analysed using UV-Vis Spectrophotometer and the samples were measured from the wavelength, 190 nm to 700 nm. Initial absorbance of dye before decolourisation treatment (I_0) and the final absorbance of dye after

treatment (F_0) were measured at λ_{max} of 597 nm. Decolourisation (%) values of the treated samples were calculated using the following equation 2 [33].

$$Decolourization\ (\%) = \frac{I_0 - F_0}{I_0} \times 100 \qquad (2)$$

FTIR analysis

Influence of acidic and alkaline pH values on dye removal (reduction / elimination of functional groups) by the composite samples was studied using Fourier-transforms infrared. Spectra were obtained between the wave numbers, 650 - 4000 cm^{-1} with a scanning rate of 32 scans per minute and resolution of $1cm^{-1}$ [34].

Result and Discussion

X-Ray diffraction and crystallinity

$$CaCO_3 \xrightarrow{\Delta\ 900\ ^\circ C} CaO + CO_2 \uparrow \qquad (3)$$

$$2Al_2Si_2O_5(OH)_4 \xrightarrow{\Delta\ 900\ ^\circ C} 2Al_2Si_2O_7 + 4H_2O \uparrow \qquad (4)$$

$$TiO_2 \xrightarrow{\Delta\ 900\ ^\circ C} TiO_2 \qquad (5)$$

$$2Al_2Si_2O_7 \xrightarrow{\Delta\ 1000\ ^\circ C} Si_3Al_4O_{12} + SiO_2 \qquad (6)$$

$$3Si_3Al_4O_{12} \xrightarrow{\Delta\ 1000\ ^\circ C} 2Si_3Al_6O_{13} + 5SiO_2 \qquad (7)$$

$$3CaO + SiO_2 + TiO_2 \xrightarrow{\Delta\ 1000\ ^\circ C} Ca_2SiO_4 + CaTiO_3 \qquad (8)$$

$$Ca_2SiO_4 + 2Ca \xrightarrow{\Delta > 1000\ ^\circ C} CaTiO_3 + Ca_3SiO_5 \qquad (9)$$

X-ray diffractograms for 2θ values ranging from 5 to 90° for raw materials and KCT composite samples with the proportions of 1:1:1, 1:2:1 and 1:1:2, calcined at temperatures 900, 1000, 1100 and 1200 °C are shown in the Fig 2 a, b and c, respectively. For samples with 1:1:1 KCT proportion, It can be observed from the diffractogram that at 900 °C, there is only surface adherence of chemicals noted and phase transformation starts from 1000 °C. Formation of metakaolinite ($Al_2Si_2O_7$) is observed in samples calcined at 900 °C as shown in equation 2 [35], and formation of Silicon dioxide (SiO_2) from kaolin is observed at 1000 °C as shown in equation 4 [36]. These formation enhances the adsorption properties of the prepared composites [37]. Further calcination at 1000 °C leads to formation of calcium titanium trioxide ($CaTiO_3$) and Ca_2SiO_4 (Belite). Formation of $CaTiO_3$ and Ca_2SiO_4 are the main phases that contributes as a photocatalyst and adsorbent respectively [24,38]. Other complex phases like Calcium aluminosilicate ($Al_2Ca_2SiO_7$), Aluminium oxide (Al_2O_3), Calcium oxide (CaO) and SiO_2 are also formed at 1100 °C due to the possible reactions [39] that can influence photocatalytic and adsorption properties of prepared composite [40]. Further calcination temperature above 1100 °C results in formation of Tricalcium silicate (Ca_3SiO_5 - Alite) phases [22]. It is observed that TiO_2 transforms from anatase phase to rutile phase above 1000 °C leading to a shift in peak as shown in Fig 2 a. This transformation can highly influence the photocatalytic activity of the prepared composite as photocatalytic activity of rutile phase is less than that of anatase phase [41].

XRD pattern shown in Fig 2 b) and c) also suggests that the same presence of these phases in KCT composite formed using 1:2:1 and 1:1:2 proportions. Compared to the TiO_2 peak found in 1:1:1 and 1:1:2 KCT composite, TiO_2 peak in 1:2:1 KCT composite calcined above 900 °C is less due to the dominancy of Calcium carbonate and Kaolin proportionately thus lowering the photocatalytic property. Following equations (3-9) list the most possible reactions that happen during calcination of KCT composites at various temperatures. At calcination temperature of 900 °C, $CaCO_3$ decomposes to CaO (Calcium oxide), Metakaolinite ($Al_2Si_2O_7$) formation is seen due to dehydroxylation of kaolin and TiO_2 seems to be stable and is shown in equation (3), (4) and (5), respectively. Formation of SiO_2, calcium titanium trioxide ($CaTiO_3$), Ca_2SiO_4 (Belite) is shown in the equations (6-9). Formation of Ca_3SiO_5 (Alite) phases is shown in equation (9). All the reactions discussed by the following equations are well in agreement with the XRD Fig 2 a, b and c.

Surface Morphology

While producing the composites, particle agglomeration was rapid as the calcination temperature was increased, regardless to the proportions of the individual components. Fig 3 shows the SEM images of raw chemicals (a-c) and KCT composites of 1:1:1, 1:2:1 and 1:1:2 proportions calcined at 900, 1000, 1100 and 1200 °C (d-o). Surface adherence of powders was visible on the samples calcined at 900 °C and at 1000 °C and the particles size of the composites increased with respect to temperature due to the formation of calcium titanium trioxide ($CaTiO_3$), Ca_2SiO_4 (Belite) and Ca_3SiO_5 (Alite) phases as shown in the equations (6-9). The changes in particle size with respect to temperature is shown in Fig 4 and a strong fusing and tightening (or hardening) of composite samples was seen with the samples calcined at 1100 and 1200 °C [42] as shown in Fig 3. Extent of agglomeration, fusing and tightening of composite structures are expected to influence surface area of the composite samples and thereby adsorption of residual dyes from the effluent [43].

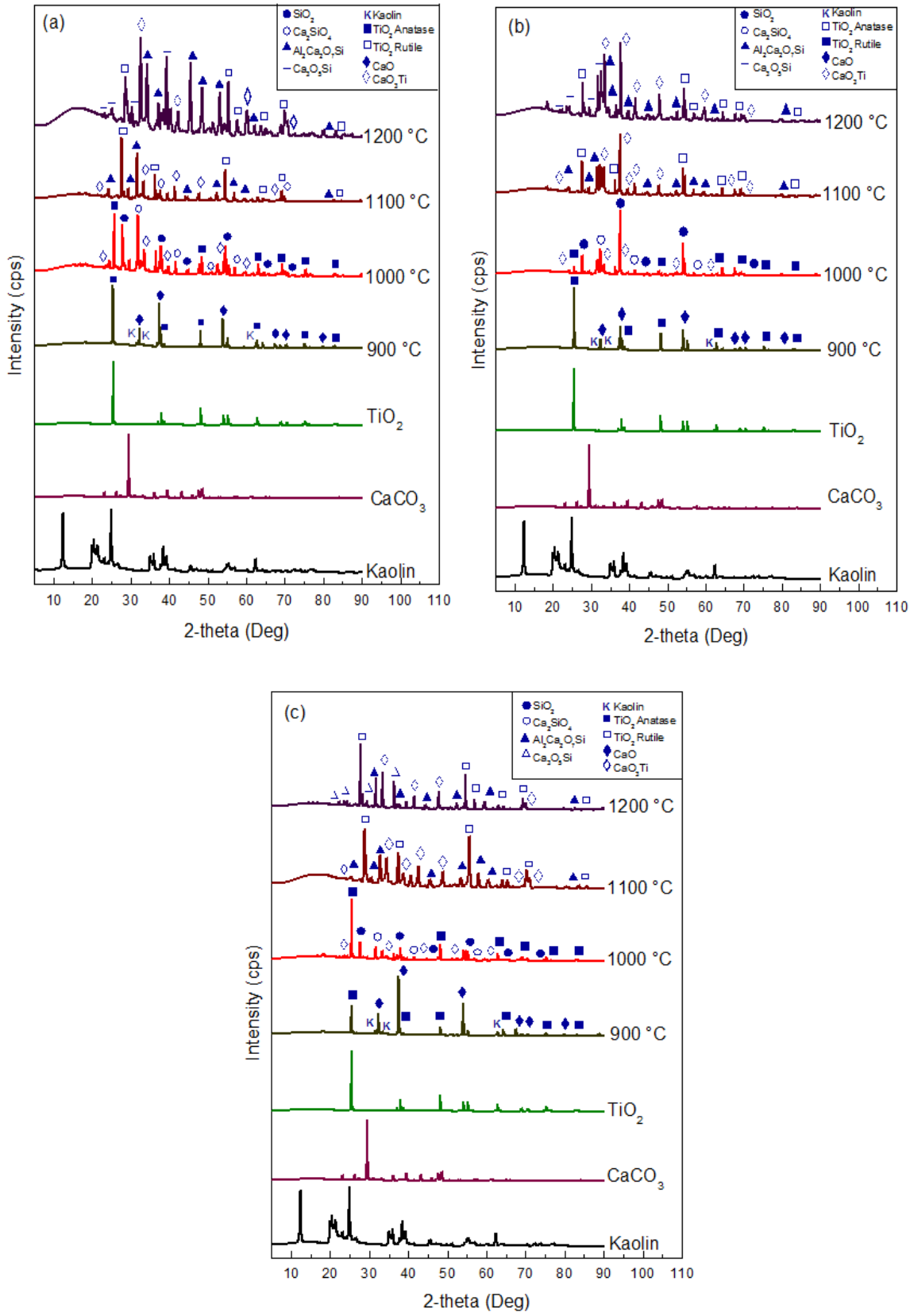

Fig. 2: X-ray diffraction of components and composites prepared at various temperatures. (a) 1:1:1, (b) 1:2:1 and (c) 1:1:2.

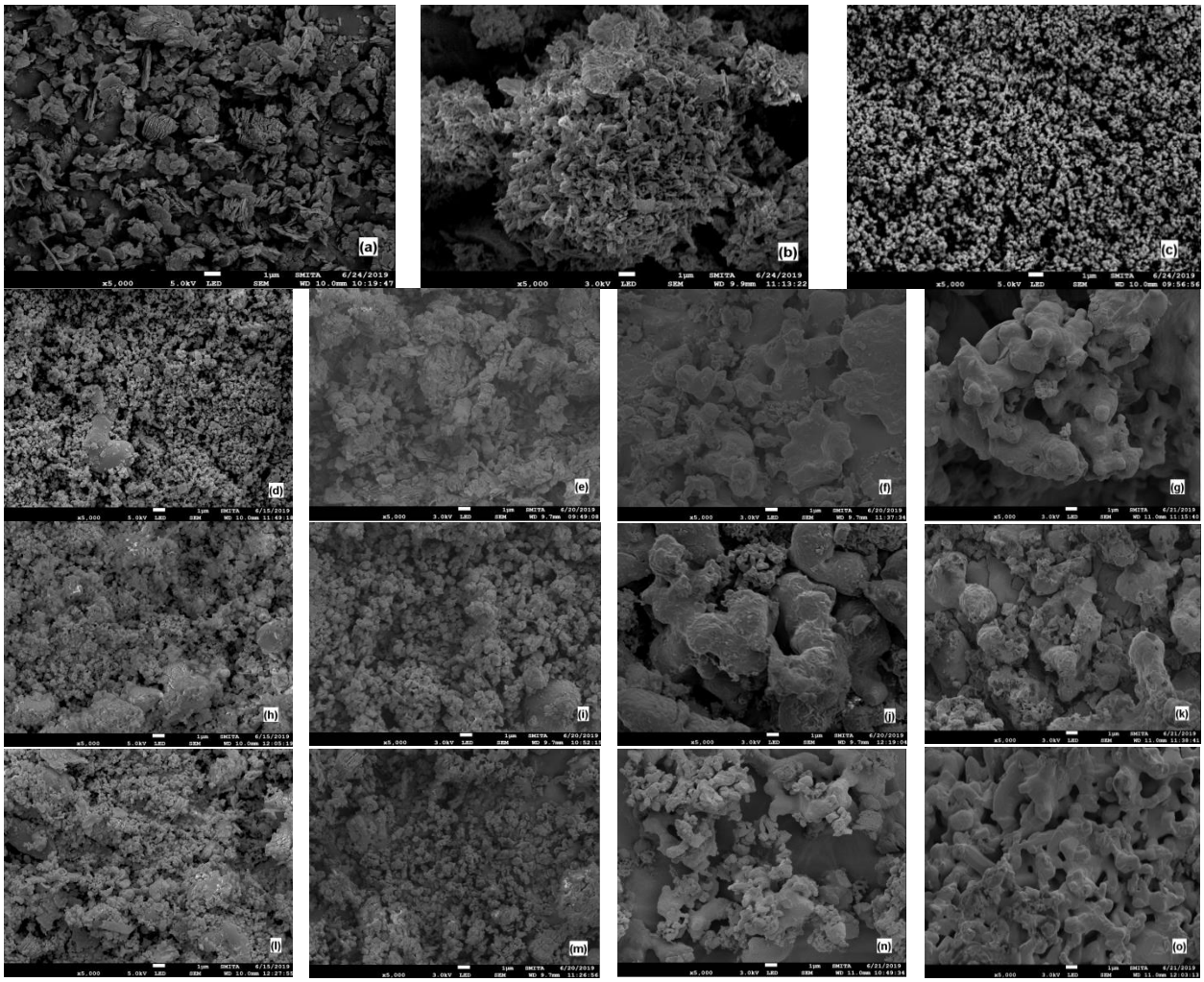

Fig. 3: Surface Morphology of (a) Kaolin, (b) $CaCO_3$, (c) TiO_2, composite samples with proportions 1:1:1, 1:2:1and 1:1:2 calcined at – 900 °C(d,h,l), 1000 °C (e,i,m), 1100 °C (f,j,n), and 1200 °C (g,k,o)

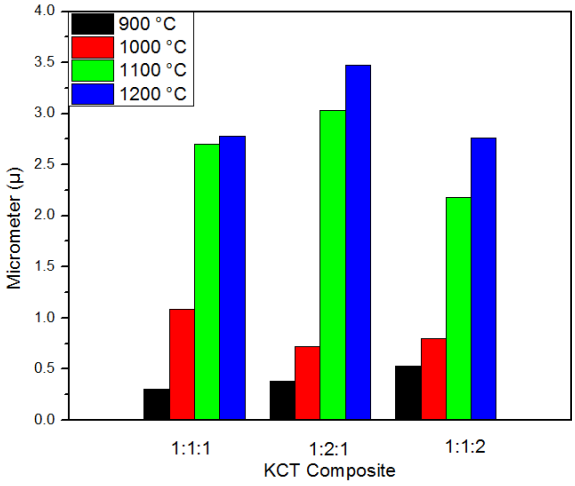

Fig. 4: Particle size of calcined composite.

Elemental Analysis

Elemental analysis of composite samples in terms of oxygen (O), titanium (Ti), aluminium (Al), silica (Si), calcium (Ca) and carbon (C) by weight (%) and chemical composition (in weight %) of components and composites are shown in the Table 1. All the composite samples showed ~50% or more of oxygen by weight than calcium, titanium, aluminium and silica, irrespective of composite proportions. Other elements in the composites were well in agreement, corresponding to the composite proportion [44].

Most possible chemical transformations, during calcination, are shown in equation (3), (4) and (5). Absence of carbon is seen in all the composites as most of them are lost in the form of carbon-di-oxide, as shown in equation (3). At 1000 °C, belite

(Ca_2SiO_4) and calcium titanate ($CaTiO_3$) are the most possible forms of chemical transformation as shown in the equations 6-9, [22,45] in which belite is expected to act as the adsorbent and calcitum titanate as a photocatalyst during degradation of dyes.

Surface area

Formations of composites using different components, having varied surface areas, are expected to have different resultant surface area and are evident from the results shown in the Table 1. Surface areas of the composite samples obtained at 1000 ºC showed the highest values compared to other temperature levels. Doping of kaolin and decarbonation of carbonate were responsible for the changes in the surface area of the samples since titanium dioxide is capable of withstanding these temperatures without degradation. Higher proportion of calcium carbonate resulted relatively high elimination of carbon dioxide on heating (Equation 3) thus facilitating high levels of fusion in the reaction. However, at very higher temperatures, i.e. >1000 °C, the particles with higher surface area started fusing (Fig 3) together thereby resulting in the reduction of surface areas [46]. Wide variation in the surface area is, definitely, expected to alter the extent of reactions during the effluent decolourisation, influencing both adsorption and photocatalysis.

Band gap

Band gap, which indicates the gap in the energy levels between valence band and conduction band, largely decides the formation of electron-hole pair in photocatalytic compounds[47]. When photocatalytic compounds are doped with other substances, the band gap is expected to change according to the nature and extent of doping, thereby alter the photocatalytic reactions. In general, larger the band gap of the composites (or any other compound), lesser will be the light absorbed and the valance band will increase thus increasing the energy levels of the composite. Higher band gap increases the oxidation power of photocatalyst and it also facilitates the electron transfer that aids in better photocatalytic activity in UV light [48]. Titanium dioxide, in its original form, shows a band gap of 3.31 eV, which increases by 11% at high temperature due to changes in its electronic structure, resulting from doping. But as the calcination temperature increases, it could be noted that, the band gap increases and remains stabilized above 1100 °C for all composite samples regardless to the proportions. During the formation of composites, the band gap increases with decrease in the surface area of particles [49] with conversion of titanium dioxide from anatase to rutile [14] phase, and subsequent heating led to reduction in surface area due to fusing of compounds together obviously resulted in higher band gap, confirming the earlier research work [49]. Band gap obtained at 1000 °C, indicates the formation of new phases like calcium titanate ($CaTiO_3$), whose band gap ranges between 3.2 – 3.4 eV and further heating of calcium titanate, beyond 1000 °C, influences the band gap adversely. However, calcium titanate, an active photocatalyst, as one of the major components in the composites, is expected to contribute towards colour removal in the effluent.

FTIR analysis on dye degradation

Chemical structure of Reactive Black 5 is shown [50] in Fig 5 a and the FTIR spectra of Reactive Black 5, its residues after treatment of effluent using composites under acidic, neutral and alkaline pH conditions are shown in Fig 5 b. Reactive Black 5 dye showed many major-sharp and minor peaks representing its constituent functional groups. FTIR spectra of original dye sample exhibited the presence of –NH stretch at 3450 cm^{-1}, CH_2 stretch at 2968 – 2888 cm^{-1}, C=N stretch at 1640 cm^{-1}, N=N stretch at 1400 – 1580 cm^{-1}, and O-C stretch at 1078 – 1256 cm^{-1} [51]. After the treatment with photocatalytic adsorbent (KCT composite), there was reduction in all the peaks, in general, to different extents under various pH conditions. There was a marked reduction in –NH stretch in the samples treated at neutral and alkaline conditions, but –NH stretch at 3000 – 3718 cm^{-1} completely disappeared in samples treated under acidic condition. Removal of –NH from the samples treated under acidic condition is in agreement with the obtained FTIR results in earlier reports [52]. The peaks from 650 – 2000 cm^{-1} decreased remarkably and formation of new peaks are seen in the samples treated in acidic, neutral and alkaline conditions, indicating C=O stretch at 1640 cm^{-1}, CH_2 stretch at 1400 cm^{-1} and C-H stretch at 710 - 984 cm^{-1}. The chromophore N=N group [53], which is the colour bearing group (1400 – 1580 cm^{-1}), is notably absent in all the three pH conditions or appeared as a very weak peak on account of substantial degradation and removal by adsorption.

Table-1: Effect of composition and calcination temperatures on surface area and band gap.

Compounds/Composites	Weight (%)						Surface Area (m^2/g)	Band Gap (eV)
	O	Ti	Al	Si	Ca	C		
Kaolin	68.6	-	15.4	16	-	-	14.629	-
$CaCO_3$	55.5	-	-	-	18.7	25.8	5.912	-
TiO_2	61.4	38.6	-	-	-	-	8.321	3.31
1:1:1 – 900 °C	63.2	27.3	3.9	3.4	2.2	-	9.114	3.35
1:2:1 – 900 °C	62.2	8.6	4.6	5.6	19.2	-	6.032	3.36
1:1:2 – 900 °C	63.4	17.9	7.4	6.6	4.6	-	9.891	3.34
1:1:1 – 1000 °C	49.3	6.1	8.6	9.3	26.7	-	15.342	3.41
1:2:1 – 1000 °C	57.0	0.5	1.2	1.0	40.3	-	10.882	3.70
1:1:2 – 1000 °C	54.0	35	3.1	2.6	5.3	-	11.225	3.39
1:1:1 – 1100 °C	57.9	1.1	9.7	9.5	21.8	-	5.609	3.68
1:2:1 – 1100 °C	49.1	1.3	6.7	6.4	36.5	-	4.747	3.66
1:1:2 – 1100 °C	57.1	31	4.5	3.8	3.6	-	5.597	3.67
1:1:1 – 1200 °C	60.0	0.5	19.1	19.7	0.7	-	4.576	3.68
1:2:1 – 1200 °C	52.6	2.7	6.6	6.0	32.2	-	5.190	3.66
1:1:2 – 1200 °C	58.9	13.4	7.5	6.7	13.5	-	3.725	3.67

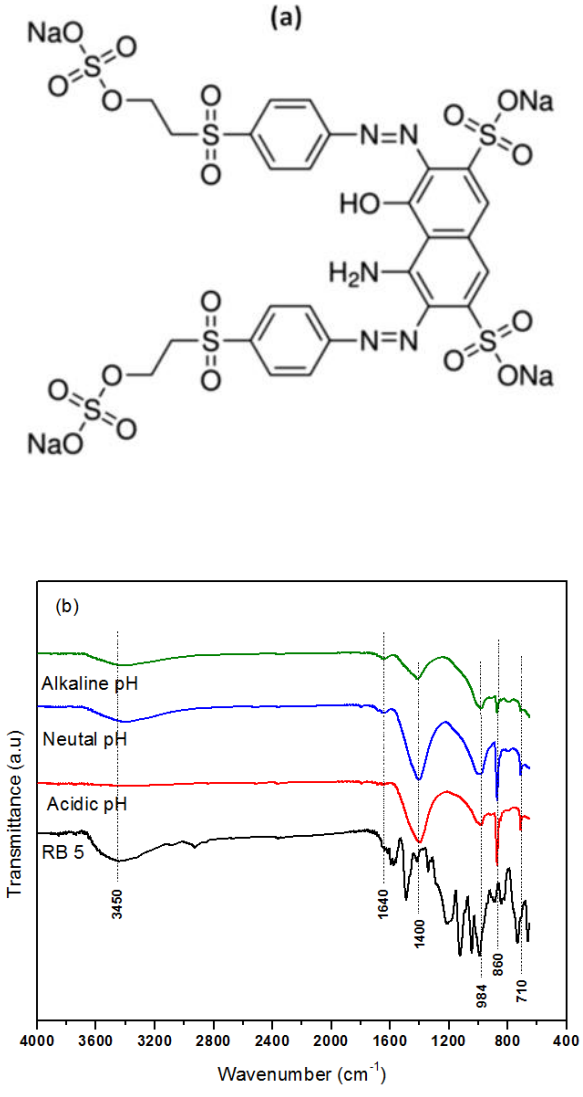

Fig. 5: (a) Chemical structure and (b) treated effluent of Reactive Black 5.

Decolourisation

Decolourisation (%) of Reactive Black 5 using 10 grams KCT without calcination in one litre of dye effluent at pH 11 for 2, 4 and 6 hours are shown in Table 2. Similarly 10 grams of KCT composites in one litre of dye effluent at pH values, 3, 5, 7, 9 and 11 for a duration of 2, 4 and 6 hours are shown in the Table 2. KCT samples without calcination showed less decolourisation efficiency at all the three proportions compared to calcined KCT composite. Phase modification and characteristics enhancement during calcination of KCT composite resulted in better decolourisation efficiency as shown in Table-2 [54]. KCT composites calcined at 1000 ˚C reported the maximum decolourisation % at pH 3 and treatment time of 6 hours. Maximum of 82.62%, 65.08% and 80.16 % colour removal is achieved in decolourising Reactive Black 5 effluents using 1:1:1, 1:2:1 and 1:1:2 respectively (Fig 6). Decolourisation efficiency with respect to calcinations temperature, pH, composite proportion and time of treatment is discussed as follows.

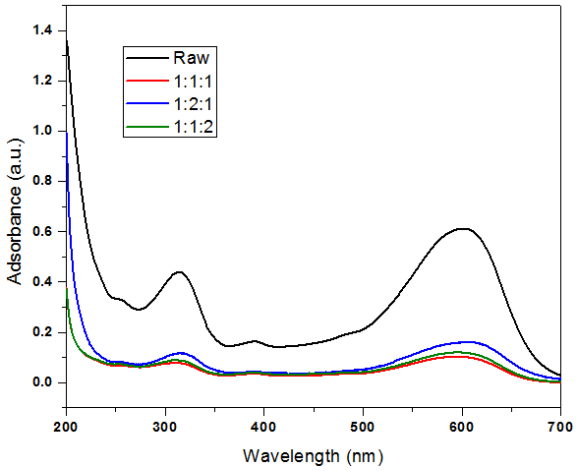

Fig. 6: Decolourisation of Reactive Black 5.

Table-2: Decolourisation of Reactive Black 5 using K-C-T composites.

KCT	pH	Decolourisation (%)			KCT	pH	Decolourisation (%)			KCT	pH	Decolourisation (%)		
		2h	4h	6h			2h	4h	6h			2h	4h	6h
1:1:1 WC	11	22.46	27.05	29.84	1:2:1 WC	11	16.07	18.36	20.66	1:1:2 WC	11	28.36	31.15	32.79
	3	51.80	75.74	76.07		3	42.30	53.44	54.75		3	52.95	73.93	74.75
	5	44.75	71.15	72.79		5	39.02	51.31	53.44		5	46.23	70.16	71.80
1:1:1 900 °C	7	39.34	64.43	65.74	1:2:1 900 °C	7	34.74	49.67	50.82	1:1:2 900 °C	7	41.64	64.92	65.08
	9	39.18	63.11	63.61		9	32.30	48.20	50.00		9	40.98	64.43	64.59
	11	39.02	62.79	62.79		11	31.48	47.05	49.34		11	40.66	64.59	64.59
	3	63.61	80.33	82.62		3	57.54	63.61	65.08		3	63.11	78.69	80.16
	5	58.69	74.10	76.56		5	54.75	59.18	60.33		5	59.67	75.57	76.72
1:1:1 1000 °C	7	55.74	71.48	73.61	1:2:1 1000 °C	7	51.31	57.21	57.87	1:1:2 1000 °C	7	56.39	73.44	73.93
	9	55.25	69.51	70.16		9	48.20	57.05	57.87		9	56.72	73.11	73.61
	11	54.75	69.02	70.16		11	46.56	57.38	57.70		11	55.08	72.79	72.95
	3	46.72	50.16	50.49		3	32.79	33.44	34.26		3	39.84	42.13	42.62
	5	40.98	47.05	48.20		5	30.66	31.48	31.97		5	37.38	40.00	40.98
1:1:1 1100 °C	7	36.86	44.43	44.59	1:2:1 1100 °C	7	30.33	30.66	31.15	1:1:2 1100 °C	7	34.43	39.02	39.84
	9	35.25	42.79	43.28		9	26.72	28.20	28.36		9	34.75	39.51	39.18
	11	35.41	42.95	43.61		11	25.90	27.05	27.87		11	33.77	38.36	38.69
	3	36.39	36.89	37.05		3	20.66	20.98	20.98		3	25.90	26.07	26.07
	5	32.13	32.79	32.95		5	19.67	20.33	20.33		5	24.26	25.25	25.90
1:1:1 1200 °C	7	30.66	30.82	30.82	1:2:1 1200 °C	7	17.87	18.36	18.36	1:1:2 1200 °C	7	23.11	23.49	23.77
	9	28.03	29.84	29.84		9	15.41	16.56	16.56		9	22.13	22.46	22.79
	11	26.72	27.05	27.87		11	16.07	16.07	16.12		11	20.98	22.13	22.46

Effect of Calcination Temperatures on Decolourisation

Decolourisation of Reactive Black 5 is highly influenced by the calcination temperatures at which the composite samples were prepared. Table 2 briefs the decolourisation performance of KCT without calcinations (WC) and KCT composite with calcinations. It could be observed from the Table 2 that the samples without calcinations show less decolourisation efficiency than calcined composites. Calcined composite enhances the new phase formation and modifies composite characteristics thus improving the performance of composite on decolourisation of RB5 [55]. As the calcination temperature increases, the decolourisation efficiency also increases up to 1000 °C followed by a sharp decrease above 1000 °C for all the proportions. This may further be supported by the XRD images that confirm the formation of $CaTiO_3$ and Ca_2SiO_4 which contributes as an effective photocatalyst and adsorbent respectively. Further SEM images (Fig 3) indicating the growth of agglomeration as the calcination temperature increases thereby affecting the surface area of the composite at temperature above 1000 °C and band gap of the photocatalyst, as detailed in Table-2.

Another potential reason for the inertness of the developed composites after 1000 °C is due to the conversion of titanium dioxide into rutile phase from anatase phase when exposed above 1000 °C. XRD images shown in Fig 2 a, b and c also confirm the transformation of anatase TiO_2 to rutile [56]. The rutile phase of the titanium dioxide is characterised by high chemical stability and low reactivity. This must be the reason for the negative impact of higher temperature composite on decolourisation besides band gap and surface area. Fig 7 a, b and c shows the effects of calcination temperatures of KCT composite samples and effluent pH on the decolourisation percentage for treatment duration of 6 hours.

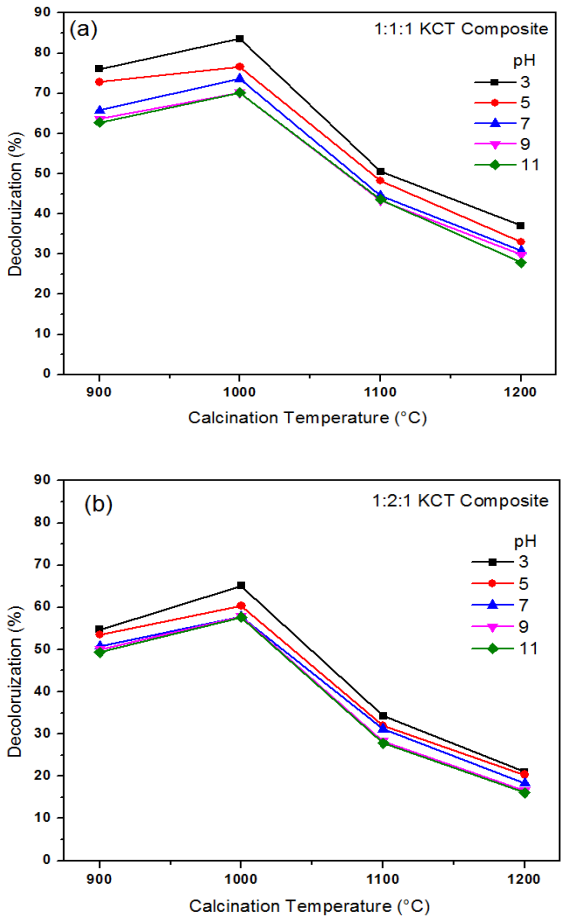

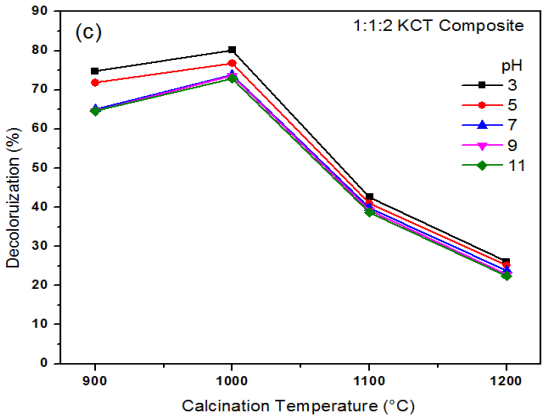

Fig. 7: Effect of composite calcination temperatures and effluent pH on decolourisation

$$CaTiO_3 + h\vartheta \rightarrow CaTiO_3 + e^- + h^+ \quad (10)$$

$$e^- + H_2O \rightarrow OH^\bullet \quad (11)$$

$$e^- + O_2 \rightarrow O_2^- \quad (12)$$

$$OH^\bullet + O_2^- + Reactive\ Black\ 5 \rightarrow Degradation\ products \quad (13)$$

$$Ca_2SiO_4 + 4H^+ \rightarrow 2Ca^{2+} + SiO_2(aq) + 2H_2O \quad (14)$$

Effect of pH on Decolourisation

Decolourisation of reactive dye effluents treated with composites at various pH values 3, 5, 7, 9 and 11 demonstrates its influence on decolourisation efficiency. All the composite samples showed good decolourisation efficiency under acidic pH than alkaline pH. Maximum decolourisation efficiency was obtained at a pH of 3, which decreased as the pH is increased till pH 7 and, further, a very minimal change was observed at pH values above 7. Calcium titanate, with the zeta potential value of 3, acts effectively in decolourisation as shown in the equation (10 – 14) thereby confirming earlier published report [54].

The acquisition of positive charge of Ca_2SiO_4 (belite) in the acidic pH promotes a large amount of calcium ions (Ca^{2+}) as shown in the equation (14). This process in turn supplements the photocatalytic activity during decolourisation process [57–59]. Further, the Anionic nature of Reactive Black 5 became highly favourable under the acidic conditions, [60] thus it promotes adsorption and photocatalytic reactions at lower pH. As shown in the above equations, calcium titanate forms the hydroxyl radical, a strong oxidizing agent in destroying colour to degradation products. Fig 8 a, b and c shows the effects of pH on decolourisation efficiency with respect to samples treated for duration of 6 hours in the UV chamber. It could be noted that minimum or no change in decolourisation percentage is noted for samples treated under neutral and alkaline pH.

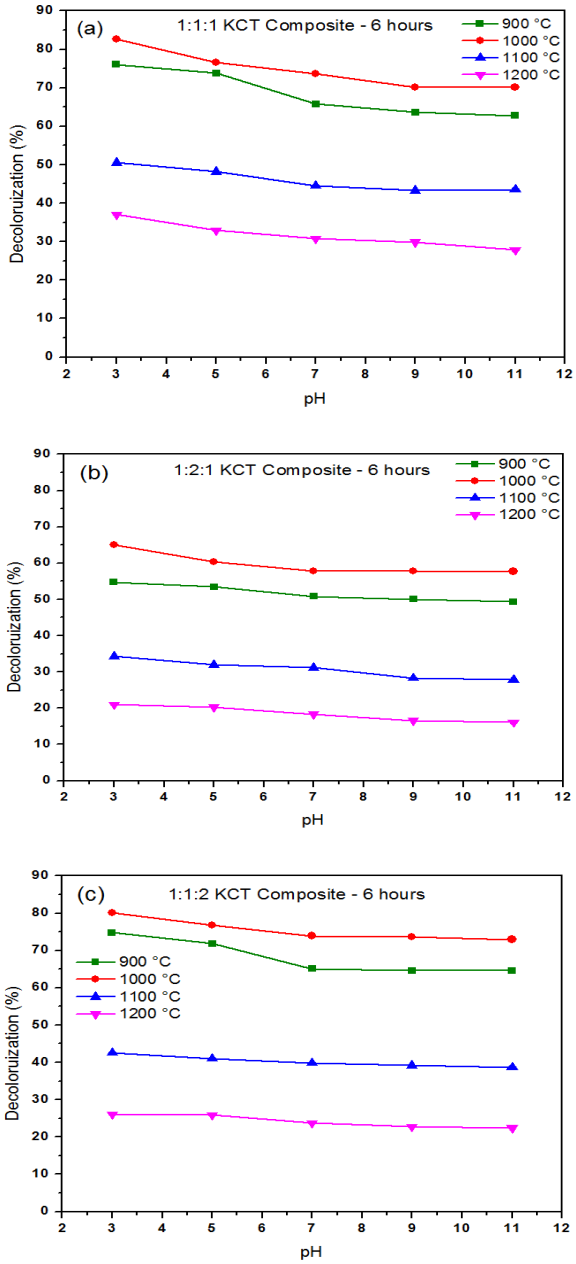

Fig. 8: Effect of pH on decolourisation efficiency.

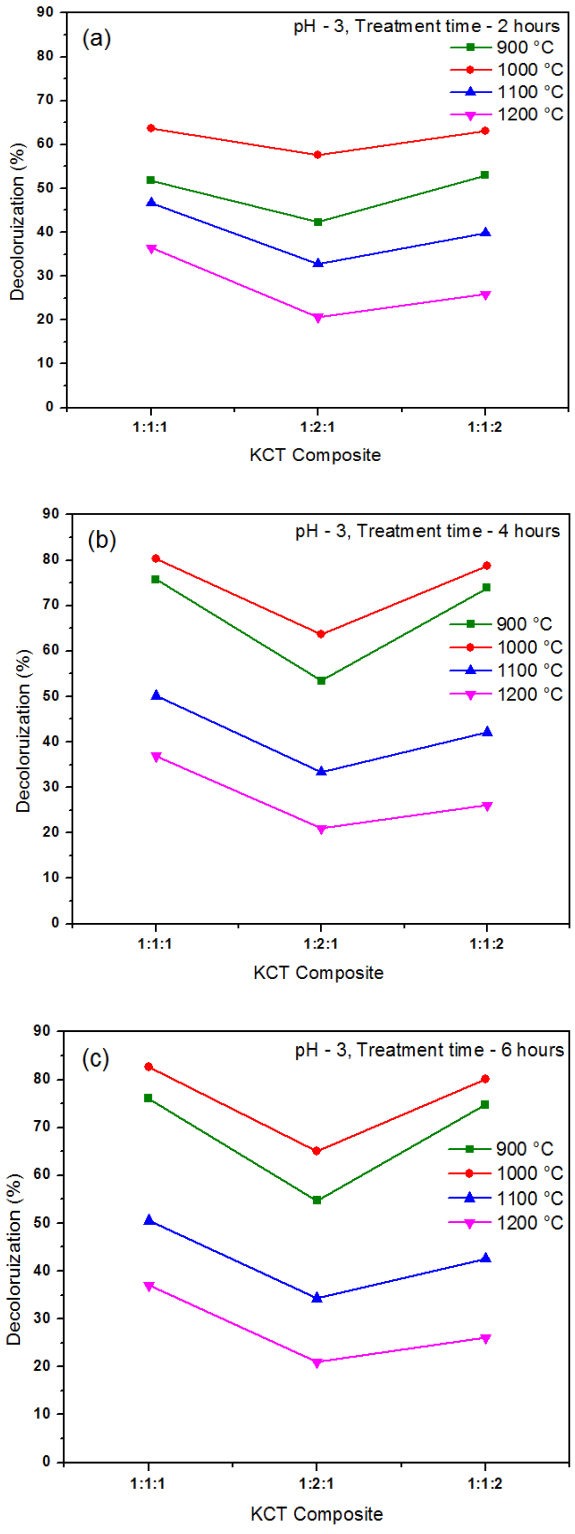

Fig. 9: Effect of composite samples on decolourisation at different pH and temperature

Effect of Composite Proportions on Decolourisation

Fig 9 a, b and c show the effect of decolourisation efficiency for those samples treated under pH 3 for a duration of 2, 4 and 6 hours using all the three proportions of KCT composites calcined at 900, 1000, 1100 and 1200 °C. KCT composites with proportion 1:2:1 exhibited a less decolourisation efficiency than the other two proportions. Among the three proportions of KCT composites, composite with proportions 1:1:1 and 1:1:2 were found to yield better decolourisation efficiency as shown in the Fig 3. When considered proportionately, the surface areas of 1:1:1 and 1:1:2 KCT composites seem to be better than 1:2:1 KCT composite samples with corresponding impact on band gap values.

Effect of Treatment Time on Decolourisation

All the composite samples seem to be effective for a treatment time of 4 hours, after which there was a marginal improvement in the decolourisation efficiency of the samples treated for 6 hours [61]. Fig 10 a, b and c show the effect of treatment time on decolourisation of effluent for samples treated at pH 3. Samples calcined at 900 and 1000 °C were found to be responsive with time from 2 hours to 4 hours. On considering the samples calcined at 1100 and 1200 °C, there was no or minimal change after 2 hours due to early saturation of the composites on account of less surface area of the composites and rutile phase of TiO_2, affecting the performance of calcium titanate.

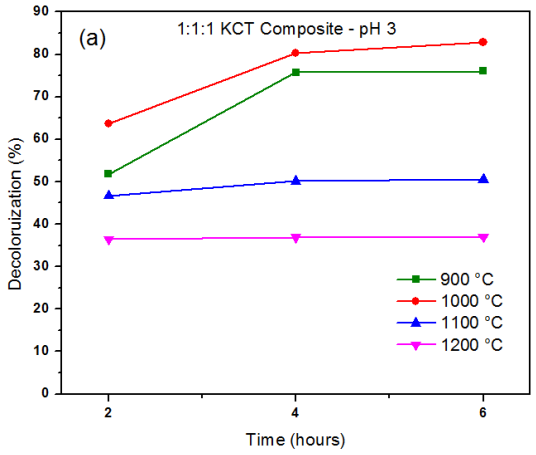

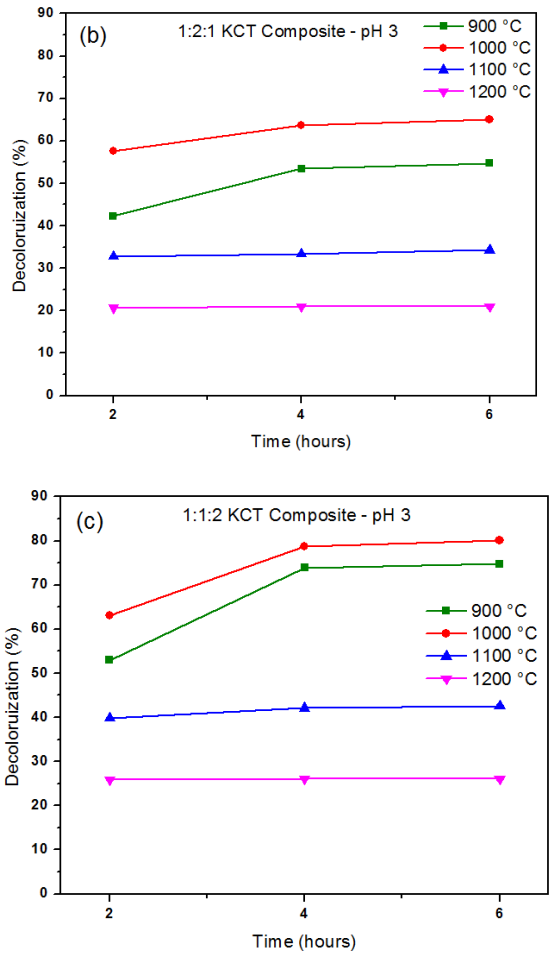

Fig. 10: Effect of treatment time on decolourisation efficiency.

Conclusion

Photocatalytic adsorbents are produced using calcination of kaolin, calcium carbonate and titanium dioxide. Calcium titanate ($CaTiO_3$) and belite (Ca_2SiO_4) were formed as the active compounds with different proportions and process conditions. Developed KCT composites (1:1:1 and 1:1:2) calcined at 1000 °C exhibited a decolouisation efficiency of 82% and 80%, respectively at pH 3. The other composites produced in the experiment (1:2:1) did not show significant decolourisation efficiency due to low surface area, high band gap together with relative stable rutile phase of titanium dioxide. Adsorptions of dyes from effluent were highly influenced by photocatalysis and pH values of the effluents. Nevertheless, the significant reduction in colour value is expected to reduce the load on subsequent treatments using chemical methods with lower sludge generation and reduced environmental impacts, which further can be reduced with optimizing the process conditions. Though the experimental results based on lab scale have resulted with good efficiency, there is a need to scale-up the treatment to larger levels at commercial operations.

Reference

1. M. D. N. Sánchez, P. M. Santos, C. P. Sappó, J. L. P. Pavón, and B. M. Cordero, Microextraction by packed sorbent and salting-out-assisted liquid-liquid extraction for the determination of aromatic amines formed from azo dyes in textiles, *Talanta*, **119**, 375 (2014).
2. B. P. Dojčinović, G. M. Roglić, B. M. Obradović, M. M. Kuraica, T. B. Tosti, M. D. Marković, and D. D. Manojlović, Decolorization of Reactive Black 5 using a Dielectric Barrier Discharge in the presence of inorganic salts, *J. Serbian Chem. Soc.*, **77**, 535 (2012).
3. T. Hadibarata, L. A. Adnan, A. R. M. Yusoff, A. Yuniarto, Rubiyatno, M. M. F. A. Zubir, A. B. Khudhair, Z. C. Teh, and M. A. Naser, Microbial decolorization of an azo dye reactive black 5 using white-rot fungus Pleurotus eryngii F032, *Water. Air. Soil Pollut.*, **224**, 1 (2013).
4. M. M. Felista, W. C. Wanyonyi, and G. Ongera, Adsorption of anionic dye (Reactive black 5) using macadamia seed Husks: Kinetics and equilibrium studies, *Sci. African*, **7**, 283 (2020).
5. C. Allègre, P. Moulin, M. Maisseu, and F. Charbit, Treatment and reuse of reactive dyeing effluents, *J. Memb. Sci.*, **269**, 15 (2006).
6. S. Mondal, Methods of dye removal from dye house effluent - An overview, *Environ. Eng. Sci.*, **25**, 383 (2008).
7. N. Abidi, E. Errais, J. Duplay, A. Berez, A. Jrad, G. Schäfer, M. Ghazi, K. Semhi, and M. Trabelsi-Ayadi, Treatment of dye-containing effluent by natural clay, *J. Clean. Prod.*, **86**, 432 (2015).
8. N. Tufekci and I. Toroz, Pollutants of Textile Industry Wastewater and Assessment of its Discharge Limits by Water Quality Standards, *Turkish J. Fish. Aquat. Sci.*, **7**, 97 (2007).
9. D. A. Yaseen and M. Scholz, *Textile dye wastewater characteristics and constituents of synthetic effluents: a critical review*, in *Int. J. Environ. Sci. Technol.*, **16**, 1 (2019).
10. A. Gul, S. Muhammad, S. Nawaz, S. Munir,

K. U. Rehman, S. Ahmad, and O. S. Humphrey, Ficus religiosa bark an efficient adsorbent for Alizarin Red S dye: Equilibrium and kinetic analysis, *J. Iran. Chem. Soc.*, **19**, 1737 (2022).
11. G. Crini and E. Lichtfouse, Advantages and disadvantages of techniques used for wastewater treatment, *Environ. Chem. Lett.*, **17**, 145 (2019).
12. S. Noor and M. B. Taj, Mixed-micellar approach for enhanced dye entrapment: A spectroscopic study, *J. Mol. Liq.*, **338**, 116701 (2021).
13. M. B. Taj, S. Noor, T. Javed, A. Ihsan, G. Sarwari, S. Jabeen, T. Sharif, Z. Naseem, I. Naz, et al., Effect of nonionic surfactant on micellization thermodynamics and spectroscopic profile of dye-surfactant aggregation, *J. Dispers. Sci. Technol.*, **1** (2021).
14. Y. U. Liang, W. Chen, G. Yang, H. A. O. Ding, X. Hou, and J. U. N. Ran, Preparation And Characterization Of TiO_2/Sericite Composite Material With Favorable Pigments Properties, *Surf. Rev. Lett.*, **26** (2019).
15. A. Kanwal, H. N. Bhatti, M. Iqbal, and S. Noreen, Basic Dye Adsorption onto Clay/$MnFe_2O_4$ Composite: A Mechanistic Study , *Water Environ. Res.*, **89**, 301 (2017).
16. Y. You, KeqiQu, Z. Huang, R. Ma, C. Shi, X. Li, D. Liu, M. Dong, and Z. Guo, Sodium alginate templated hydroxyapatite/calcium silicate composite adsorbents for efficient dye removal from polluted water, *Int. J. Biol. Macromol.*, **141**, 1035 (2019).
17. H. Hassena, Photocatalytic Degradation of Methylene Blue by Using Al_2O_3/Fe_2O_3 Nano Composite under Visible Light, *Mod. Chem. Appl.*, **4**, 3 (2016).
18. M. Bhuvaneshwari, V. Thiagarajan, P. Nemade, and N. Chandrasekaran, Toxicity and trophic transfer of P25 TiO_2 NPs from Dunaliella salina to Artemia salina: Effect of dietary and waterborne exposure, 39 (2018).
19. V. Thiagarajan, L. Natarajan, R. Seenivasan, N. Chandrasekaran, and A. Mukherjee, Tetracycline affects the toxicity of P25 n-TiO_2 towards marine microalgae (2019).
20. K. Mamulová Kutlákova, J. Tokarský, P. Kovář, S. Vojtěšková, A. Kovářová, B. Smetana, J. Kukutschová, P. Čapková, and V. Matějka, Preparation and characterization of photoactive composite kaolinite/TiO2, *J. Hazard. Mater.*, **188**, 212 (2011).
21. N. R. Lakkimsetty, Study on Minimizing CO 2 Emissions in Clinker Unit of Cement Plant in Sultanate of Oman (2020).
22. H. Kamarudin, A. M. M. Al Bakri, M. Luqman, I. K. Nizar, and C. Y. H. Constru, Processing and characterization of calcined kaolin cement powderY . M . Liew , (2011).
23. B. V. Hassas, F. Boylu, and M. S. Celik, Calcined Kaolin and Calcite as a Pigment and Substitute for TiO2 in Water calcined kaolin and calcite as a pigment and substitute for tio 2 in water based paints (2011).
24. V. Petrovic, Synthesis calcium-titanate ($CaTiO_3$), *Adv. Sch. Electr. Eng.*
25. M. A. Tantawy, Cement from White Sand and Lime, 1351 (2014).
26. J. Wang, Y. Gao, L. Zhu, X. Gu, H. Dou, and L. Pei, Dyeing property and adsorption kinetics of reactive dyes for cotton textiles in salt-free non-aqueous dyeing systems, *Polymers (Basel).*, **10** (2018).
27. S. K. Ponnusamy, Enhanced photocatalytic decolorization of reactive red by sonocatalysis using TiO_2 catalyst: factorial design of experiments (2018).
28. C. Sahunin and J. Kaewboran, Treatment of Textile Dyeing Wastewater by Photo Oxidation using UV / H_2O_2 / Fe_{2+} Reagents, 181 (2006).
29. J. A. Kaduk, Crystallographic databases and powder diffraction, 304 (2019).
30. M. S. El-geundi, E. A. Ashour, R. M. A. Abobeah, and N. Shehata, IJSETR ,**3** (2014).
31. K. Natarajan, H. C. Bajaj, and R. J. Tayade, Journal of Industrial and Engineering Chemistry Photocatalytic efficiency of bismuth oxyhalide (Br , Cl and I) nanoplates for RhB dye degradation under LED irradiation, *J. Ind. Eng. Chem.*, **34**, 146 (2016).
32. Z. Zeng, W. Zhang, D. M. Arvapalli, B. Bloom, A. Sheardy, T. Mabe, Y. Liu, Z. Ji, H. Chevva, et al., A fluorescence-electrochemical study of carbon nanodots (CNDs) in bio- and photoelectronic applications and energy gap investigation, *Phys. Chem. Chem. Phys.*, **19**, 20101 (2017).
33. A. Garg, V. K. Sangal, and P. K. Bajpai, Decolorization and degradation of Reactive Black 5 dye by photocatalysis: modeling, optimization and kinetic study, *Desalin. Water Treat.*, **57**, 18003 (2016).
34. W. Ben Mbarek, M. Azabou, E. Pineda, N. Fiol, L. Escoda, J. J. Suñol, and M. Khitouni, Rapid degradation of azo-dye using Mn-Al powders produced by ball-milling, *RSC Adv.*, **7**, 12620 (2017).
35. N. Salahudeen, A. S. Ahmed, A. Al-

muhtaseb, and M. Dauda, Synthesis and Characterization of Micro - Sized Silica from Kankara Kaolin (2015).
36. S. Yuan, Y. Li, Y. Han, P. Gao, and G. Gong, Investigation on Calcination Behaviors of Coal Gangue by Fluidized Calcination in Comparison with Static Calcination, 1 (2017).
37. T. A. Aragaw and F. T. Angerasa, Heliyon Synthesis and characterization of Ethiopian kaolin for the removal of basic yellow (BY 28) dye from aqueous solution as a potential adsorbent, **6**, e04975 (2020).
38. H. C. Trivedi, V. M. Patel, and R. D. Patel, Adsorption of cellulose triacetate on calcium silicate, *Eur. Polym. J.*, **9**, 525 (1973).
39. A. Guatame-García, M. Buxton, F. Deon, C. Lievens, and C. Hecker, Toward an on-line characterization of kaolin calcination process using short-wave infrared spectroscopy, *Miner. Process. Extr. Metall. Rev.*, **39**, 420 (2018).
40. H. Dongbo, Quantitative Phase Analysis of the Calcium Silicate Slag as the Residue of Extracting Alumina from High-Alumina Fly Ash, 729 (2016).
41. C. E. Zubieta, P. V Messina, and P. C. Schulz, Photocatalytic degradation of acridine dyes using anatase and rutile TiO 2, *J. Environ. Manage.*, **101**, 1 (2012).
42. N. M. Ahmed, Comparative study on the role of kaolin, calcined kaolin and chemically treated kaolin in alkyd based paints for protection of steel, *Pigment Resin Technol.*, **42**, 3 (2013).
43. Y. Liu and Y. Yang, Evolution of the Surface Area of Limestone during Calcination and Sintering, *J. Power Energy Eng.*, **03**, 56 (2015).
44. C. Savaş Uygur, B. Pişkin, and M. K. Aydinol,Synthesis of Cathodes Lix(Ni0.80Co0.15Al0.05)O_2 with Deficient and Ex-cess Lithium Using Ultrasonic Sound Assisted Co-Precipitation Meth-od for Li-Ion Batteries, *Bull. Mater. Sci*, 1 (2017).
45. F. Z. Haque, R. Nandanwar, and P. Singh, Optik Evaluating photodegradation properties of anatase and rutile TiO 2 nanoparticles for organic compounds, *Opt. - Int. J. Light Electron Opt.*, **128**, 191 (2017).
46. N. Li, B. Yang, L. Xu, G. Xu, W. Sun, and S. Yu, Simple synthesis of Cu2O/Na-bentonite composites and their excellent photocatalytic properties in treating methyl orange solution, *Ceram. Int.*, **42**, 5979 (2016).
47. E. M. Samsudin and S. B. Abd Hamid, Effect of band gap engineering in anionic-doped TiO 2 photocatalyst, *Appl. Surf. Sci.*, **391**, 326 (2017).
48. O. R. Fonseca-Cervantes, A. Pérez-Larios, V. H. Romero Arellano, B. Sulbaran-Rangel, and C. A. G. González, Effects in band gap for photocatalysis in TiO2 support by adding gold and ruthenium, **8** (2020).
49. H. Lin, C. P. Huang, W. Li, C. Ni, S. I. Shah, and Y. H. Tseng, Size dependency of nanocrystalline TiO2 on its optical property and photocatalytic reactivity exemplified by 2-chlorophenol, *Appl. Catal. B Environ.*, **68**, 1 (2006).
50. N. M. Mokhtar, W. J. Lau, and A. F. Ismail, Dye wastewater treatment by direct contact membrane distillation using polyvinylidene fluoride hollow fiber membranes, *J. Polym. Eng.*, **35**, 471 (2015).
51. P. J. Larkin, General Outline for IR and Raman Spectral Interpretation, *Infrared Raman Spectrosc.*, 135 (2018).
52. M. El Bouraie and W. S. El Din, Biodegradation of Reactive Black 5 by Aeromonas hydrophila strain isolated from dye-contaminated textile wastewater, *Sustain. Environ. Res.*, **26**, 209 (2016).
53. S. B. Jadhav, S. N. Surwase, D. C. Kalyani, R. G. Gurav, and J. P. Jadhav, Biodecolorization of azo dye remazol orange by pseudomonas aeruginosa BCH and toxicity (Oxidative stress) reduction in allium cepa root cells, *Appl. Biochem. Biotechnol.*, **168**, 1319 (2012).
54. S. Akbar Hosseini, Preparation and characterization of calcium titanate nanoparticles with the aid of different acids and study of their photocatalytic properties, *J. Mater. Sci. Mater. Electron.*, **28**, 3703 (2017).
55. W. Ali, H. Ullah, A. Zada, M. K. Alamgir, W. Muhammad, M. J. Ahmad, and A. Nadhman, Effect of calcination temperature on the photoactivities of ZnO/SnO2 nanocomposites for the degradation of methyl orange, *Mater. Chem. Phys.*, **213**, 259 (2018).
56. P. I. Gouma and M. J. Mills, Anatase-to-Rutile Transformation in Titania Powders, *J. Am. Ceram. Soc.*, **84**, 619 (2001).
57. R. Tamayo, R. Espinoza-González, F. Gracia, U. P. Rodrigues-Filho, M. Flores, and E. Sacari, As(III) removal from aqueous solution by calcium titanate nanoparticles prepared by the sol gel method, **9** (2019).
58. Y. Kuwahara and H. Yamashita, Phosphate removal from aqueous solutions using

calcium silicate hydrate prepared from blast furnace slag, *ISIJ Int.*, **57**, 1657 (2017).
59. S. A. Carroll, W. W. McNab, and S. C. Torres, Experimental Study of Cement - Sandstone/Shale - Brine - CO 2Interactions, *Geochem. Trans.*, **12**, 1 (2011).
60. J. E. Aguiar, B. T. C. Bezerra, A. C. A. Siqueira, D. Barrera, K. Sapag, D. C. S. Azevedo, S. M. P. Lucena, and I. J. Silva, Improvement in the Adsorption of Anionic and Cationic Dyes from Aqueous Solutions: A Comparative Study using Aluminium Pillared Clays and Activated Carbon, *Sep. Sci. Technol.*, **49**, 741 (2014).
61. Y. Yan, H. Yang, X. Zhao, R. Li, and X. Wang, Enhanced photocatalytic activity of surface disorder-engineered $CaTiO_3$, *Mater. Res. Bull.*, **105**, 286 (2018).